

Assessment of cardiac iron deposition in sickle cell disease using 3.0 Tesla MRI

El-Sayed H Ibrahim¹, Fauzia Rana², Kevin Johnson¹, and Richard White¹

¹Department of Radiology, University of Florida, Jacksonville, FL, United States, ²Department of Medicine, University of Florida, Jacksonville, FL, United States

Introduction: Sickle cell disease (SCD) is an autosomal genetic blood disorder, which is one of the most common hemoglobinopathies worldwide [1]. Transfusion therapy is at present time the most accepted treatment for anemia due to SCD. However, repeated transfusions often lead to iron overload with progressive organ toxicity. Specifically, iron deposition-related cardiac dysfunction, leading to heart failure, is the main cause of death in these patients. Fortunately, cardiomyopathy due to iron overload is largely reversible if detected early enough for prompt initiation of intensive chelation therapy, which necessitates careful cardiac iron content monitoring to prevent subclinical cardiac deteriorations. Serum ferritin level is commonly measured for assessing total body iron overload. However, ferritin level is affected by liver disease activity, inflammation or infection, and may not directly reflect cardiac involvement. Liver biopsy is invasive and its accuracy is affected by heterogeneous iron deposition. Cardiac iron content can be directly measured by endomyocardial biopsy, but this method is not common because of its invasiveness and related complications. MRI measurement of transverse relaxivity rate $R2^*$ ($=1/T2^*$) at 1.5T has been established as an alternative to tissue biopsy for evaluating cardiac iron overload [2], where mean normal myocardial $T2^*$ of 52 ms has been reported. However, $R2^*$ measurement at 1.5T has low sensitivity for quantitative iron assessment. The recent rapid growth in use of 3.0T MRI scanners for clinical applications raises the question whether quantitative iron assessment will be possible at 3.0T, and what advantages are expected. The present study: 1. tests the feasibility of assessing iron concentration at 3.0T using $R2^*$, and compares the results to those acquired at 1.5T using calibrated phantoms and optimized pulse sequences; and 2. examines the implementation of the optimized 3.0T technique for assessing myocardial iron content in SCD.

Methods: Ten gel-based phantoms were prepared with different iron concentrations (0–225 $\mu\text{mol/g}$) were created and imaged with optimized $T2^*$ -weighted sequence on Siemens 1.5T and 3.0T scanners (Fig. 1). The imaging parameters for the optimized 3.0T pulse sequence were: TR = 200 ms, matrix = 256 \times 192, BW = 1776 Hz/pixel, flip angle = 20°, FOV = 380 \times 285 mm², slice thickness = 10 mm, 10 echoes (TE = 1.91–21.83 ms), and total acquisition time = 15 s. $T2^*$ was measured from the resulting images using monoexponential curve fitting, and $R2^* = 1000/T2^*$ was calculated. Regression analysis was conducted to study the relationships between $R2^*$ at 1.5T, $R2^*$ at 3.0T, and iron concentration in the phantoms. The optimized 3.0T sequence was also tested on nine SCD patients. Mid-ventricular short-axis heart slices at late diastole, and mid-liver transaxial slices were acquired (Fig. 2). Average signal intensities were measured for regions of interest inside the heart (septal wall, which suffers less susceptibility artifacts than lateral wall) and liver (away from blood vessels), from which $R2^*$ was measured as in the phantom experiments. Regression analysis was conducted to study the relationships between myocardial $R2^*$, liver $R2^*$, and serum ferritin. The phantom and patient images were analyzed by two experts to measure inter-observer variability for calculating $R2^*$. Furthermore, the analysis of the patient images was repeated by the first expert, with two weeks in-between the two analyses, to measure intra-observer variability. Bland-Altman analysis was conducted to measure the significance of measurement differences.

Results: In the phantom experiments, $R2^*$ values at 3.0T were about double of those at 1.5T (mean ratio = 1.9). At 1.5T/3.0T, $R2^*(T2^*)$ ranged from 50.7/112.4 s⁻¹ (19.7/8.9 ms) to 158.7/344.8 s⁻¹ (6.3/2.9 ms) at iron concentrations of 50 and 225 $\mu\text{mol/g}$, respectively. $T2^*$ and $R2^*$ showed decreasing nonlinear and increasing linear (correlation coefficient, $r = 0.98/0.99$) relationships, respectively, with iron concentration (Fig. 1). At 1.5T, $R2^*$ of the lowest iron concentration phantom (25 $\mu\text{mol/g}$) was almost zero. However, $R2^*(T2^*)$ of this phantom was 34.8 s⁻¹ (28.7 ms) at 3.0T, which was in agreement with the established linear relationship ($r = 0.99$) between $R2^*$ measurements and iron concentration. Bland-Altman analysis showed no bias between repeated $R2^*$ measurements in the phantoms, as all the differences lied within the two standard deviation (2SD) limit. The measurements differences (mean \pm SD) = 0.87 \pm 3.5 s⁻¹ and 2.6 \pm 6.2 s⁻¹ at 1.5T and 3.0T, respectively. In patients, myocardial/hepatic $R2^*(T2^*)$ ranged from 32.6/78.7 s⁻¹ (30.7/12.7 ms) to 78.1/243.9 s⁻¹ (12.8/4.1 ms). The patients' serum ferritin ranged from 50 to 3162 ng/ml. Myocardial $R2^*$ showed weak ($r = 0.78$) and strong ($r = 0.91$) correlations with hepatic $R2^*$ and serum ferritin, respectively. Hepatic $R2^*$ had weak correlation with serum ferritin ($r = 0.66$). Bland-Altman analysis showed good agreements between repeated myocardial $R2^*$ measurements (measurements differences / $r = -1.23\pm 6.3$ s⁻¹ / 0.92 and 0.68 \pm 5.1 s⁻¹ / 0.97 for inter- and intra-observer, respectively). The hepatic $R2^*$ inter- and intra-observer measurements showed larger variations (measurements differences / $r = -15.7\pm 26.2$ s⁻¹ / 0.97 and 9.5 \pm 16.3 s⁻¹ / 0.99 for inter- and intra-observer, respectively).

Discussion: $R2^*$ imaging at 3.0T enabled assessment of wide range of iron concentrations, as high-field imaging enabled sensitive assessment of iron overload. Typically, high-field imaging is necessary when tissue iron concentration is low and high spatial resolution is required. However, it requires perfect shimming and very short echo times to capture an appreciable signal before it rapidly decays to the noise level. Bland-Altman analysis showed low variability between repeated measurements of $R2^*$, which demonstrates the technique reproducibility for evaluating iron overload at 3.0T. The significantly larger values of hepatic $R2^*$ compared to myocardial $R2^*$ indicates an early iron deposition in the liver before it extends to the heart. The weak correlation noted between myocardial and hepatic $R2^*$ has been previously reported [3], and is attributable to the difference in iron absorption mechanism between the two organs. The good correlation between myocardial $R2^*$ and serum ferritin confirms that serum ferritin provides estimate of total body iron balance and correlates with $R2^*$ in absence of liver disease, inflammation, or infection. However, this relationship should be interpreted with caution as recent studies showed that serum ferritin level, by itself, is not a reliable indicator of cardiac iron overload, and it could have weak or non-significant relationship with $R2^*$ [4]. In conclusion, $R2^*$ measurement at 3.0T is promising technique for assessing cardiac iron overload in SCD with high sensitivity and reproducibility. In conclusion, MRI $R2^*$ measurement at 3.0T is a promising technique for direct assessment of cardiac iron overload in SCD patients with high sensitivity and reproducibility. The technique can be added to a routine cardiac MRI exam, such that both the heart function and iron overload information are obtained in the same MRI session for SCD patients. The technique can be used for preclinical diagnosis of cardiac iron overload, which is expected to improve survival in this group of patients.

References: [1] Covitz et al, Chest 1995, 108: 1214-1219.

[3] Anderson et al, Eur Heart J 2001, 22: 2171-2179.

[2] Mavrogeni et al, Eur J Haematol 2005, 75: 241-247.

[4] Kolnagou et al, Hemoglobin 2009, 33: 312-322.

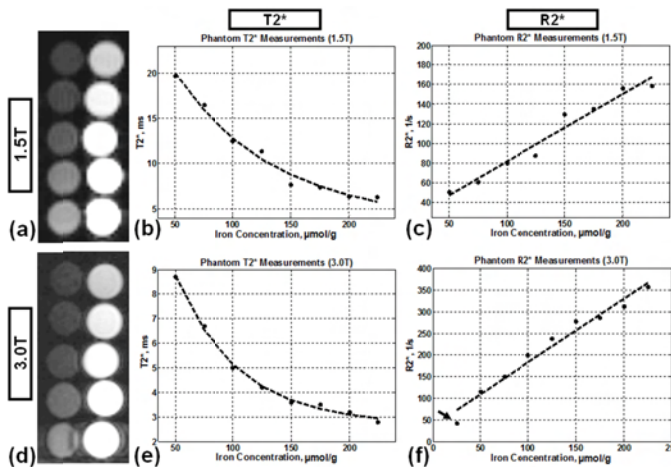


Figure 1. Phantom experiments. Calibrated iron phantoms imaged with $T2^*$ sequence at 1.5T (a) and 3.0T (d). Phantom $T2^*$ (b,e) and $R2^*$ (c,f) measurements versus iron concentration at 1.5T (b,c) and 3.0T (e,f). Arrow in panel (f) points to phantom with lowest iron concentration.

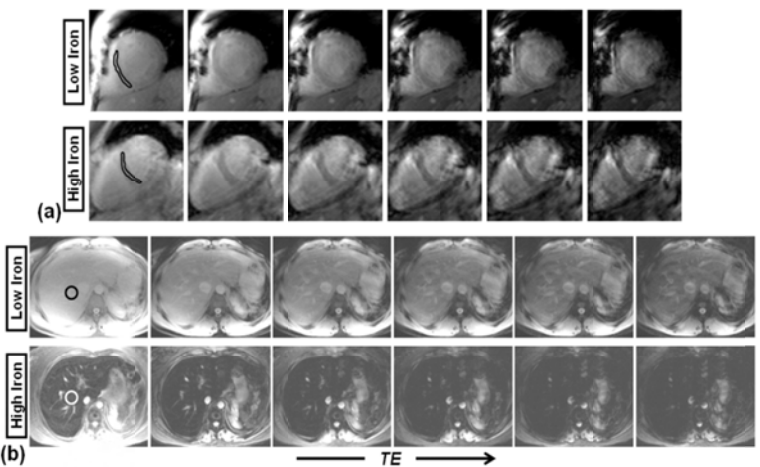


Figure 2. $T2^*$ -weighted mid-ventricular cardiac short-axis (a), and transaxial mid-liver (b) slices, acquired at different echo times (TE). Upper and lower rows show patients with low and high iron overloads (ROI are shown). Patients with high iron content show rapid decrease of signal intensity.